Fenofibrate, a PPARα agonist, has renoprotective effects in mice by enhancing renal lipolysis

Yuki Tanaka[1], Shinji Kume[1], Shin-ichi Araki[1], Keiji Isshiki[1], Masami Chin-Kanasaki[1], Masayoshi Sakaguchi[1], Toshiro Sugimoto[1], Daisuke Koya[2], Masakazu Haneda[3], Atsunori Kashiwagi[1], Hiroshi Maegawa[1] and Takashi Uzu[1]

[1]Department of Medicine, Shiga University of Medical Science, Shiga, Japan; [2]Division of Endocrinology & Metabolism, Kanazawa Medical University, Ishikawa, Japan and [3]Second Department of Medicine, Asahikawa Medical College, Hokkaido, Japan

As renal lipotoxicity can lead to chronic kidney disease (CKD), we examined the role of peroxisome proliferator-activated receptor (PPAR)-α, a positive regulator of renal lipolysis. Feeding mice a high-fat diet induced glomerular injury, and treating them with fenofibrate, a PPARα agonist, increased the expression of lipolytic enzymes and reduced lipid accumulation and oxidative stress in glomeruli, while inhibiting the development of albuminuria and glomerular fibrosis. In mice given an overload of free fatty acid-bound albumin to induce tubulointerstitial injury, fenofibrate attenuated the development of oxidative stress, macrophage infiltration, and fibrosis, and enhanced lipolysis in the renal interstitium. Fenofibrate inhibited palmitate-induced expression of profibrotic plasminogen activator inhibitor-1 (PAI-1) in cultured mesangial cells, and the expression of both monocyte chemoattractant protein-1 and PAI-1 in proximal tubular cells along with the overexpression of lipolytic enzymes. Thus, fenofibrate can attenuate lipotoxicity-induced glomerular and tubulointerstitial injuries, with enhancement of renal lipolysis. Whether amelioration of renal lipotoxicity by PPARα agonists will turn out to be a useful strategy against CKD will require direct testing.

Kidney International (2011) **79,** 871–882; doi:10.1038/ki.2010.530; published online 26 January 2011

KEYWORDS: chronic kidney disease; lipolytic enzymes; pathophysiology; renal lipotoxicity

Correspondence: *Shinji Kume, Department of Medicine, Shiga University of Medical Science, Seta, Otsu, Shiga 520-2192, Japan.*
E-mail: skume@belle.shiga-med.ac.jp

Received 16 March 2010; revised 15 October 2010; accepted 10 November 2010; published online 26 January 2011

The prevalence of chronic kidney disease (CKD) and subsequent end-stage kidney disease continues to increase worldwide, despite the application of various intensive therapy programs such as antihypertensive therapy.[1] Thus, the establishment of new therapeutic strategies is urgently required.

Lipotoxicity is an important pathogenic process in several types and stages of CKD.[2,3] Lipotoxicity in glomeruli is involved in the initiation of glomerular damage related to obesity and type 2 diabetes.[4,5] Glomerular lesion such as glomerulosclerosis and albuminuria are observed in the early stage of kidney disease associated with metabolic abnormalities. We and others have shown that intrarenal lipotoxicity resulting from enhanced renal lipogenesis and suppressed renal lipolysis contributes to the development of glomerular lesions in several animal experimental models, such as high-fat diet (HFD)-induced obese mice[6] and type 2 diabetic *db/db* mice.[7] Thus, therapeutic measures to combat lipolysis in glomerular cells may be beneficial in glomerular injury associated with metabolic syndrome or obesity.

Another type of lipotoxicity is related to the development of tubulointerstitial lesion in proteinuric kidney disease regardless of metabolic syndrome and obesity.[8] The reuptake of free fatty acid (FFA)-bound albumin, which is filtrated through the glomeruli, has been demonstrated to mediate tubulointerstitial damage in proteinuric kidney disease.[9,10] As the progressive nature of proteinuric kidney disease is dependent on the degree of tubulointerstitial damage,[11] amelioration of tubulointerstitial lipotoxicity mediated by FFA could represent an additional therapeutic target to prevent the progression of tubulointerstitial lesion in proteinuric kidney disease.

Peroxisome proliferator-activated receptor (PPAR)-α is a member of the nuclear hormone receptor superfamily of ligand-activated transcription factors, and positively regulates fatty acid β-oxidation, lipolysis, through the upregulation of expression levels of several enzymes involved in lipolysis.[12–14] PPARα exists in both glomerular and renal tubular cells, and regulates renal lipolysis.[15] Thus, the pharmacological activation of PPARα in the kidney may have a therapeutic potency through its lipolytic effect against lipotoxicity—related both to glomerular injury associated with metabolic abnormalities and to tubulointerstitial injury in proteinuric kidney disease.

In the present study, we investigated whether fenofibrate, a PPARα agonist, attenuates glomerular injury in HFD-fed obese mice and tubulointerstitial injury in a mouse model of FFA-bound bovine serum albumin (BSA)-overload nephropathy. In addition, we performed *in vitro* studies using cultured mouse mesangial and proximal tubular cells to show the direct renoprotective role of PPARα agonist. The results showed that PPARα agonist attenuated lipotoxicity-mediated oxidative stress and renal injury with enhancement of renal lipolysis, suggesting its potential use in a new therapeutic strategy against the initiation and progression of CKD.

RESULTS

Fenofibrate attenuates HFD-induced glomerular injury

At the end of the 12-week experimental period, treatment of HFD-fed obese mice with fenofibrate significantly reduced body weight, blood glucose, and plasma insulin levels, without affecting the food intake (Table 1). Furthermore, fenofibrate treatment significantly improved HFD-induced insulin resistance determined by intraperitoneal insulin tolerance test (Table 1). Fenofibrate treatment significantly decreased the plasma levels of triglyceride, although it did not affect the plasma levels of cholesterol and FFA (Table 1). No significant difference in systolic blood pressure was observed among all groups of mice (Table 1).

Next, we examined the effect of fenofibrate on HFD-induced renal injury. Fenofibrate treatment significantly attenuated the development of albuminuria in HFD-fed mice (Table 1). Histologically, fenofibrate treatment significantly attenuated HFD-induced increases of mesangial matrix area (Figure 1a and b) and glomerular volume (Figure 1a and c). Fenofibrate treatment also ameliorated glomerular fibrosis determined by immunostaining for fibronectin (Figure 1d and e), type I collagen (Figure 1f and g), and type IV collagen (Figure 1h and i). Furthermore, fenofibrate treatment significantly inhibited HFD-induced increases of mRNA expression levels of fibronectin and plasminogen activator inhibitor-1 (PAI-1) in the renal cortex, both of which are indices of renal fibrosis (Table 2). Neither HFD feeding nor fenofibrate treatment influenced *PPARα* gene expression in the renal cortex (Table 2).

Fenofibrate enhances renal lipolysis and attenuates oxidative stress in the kidney of HFD-fed mice

Oil-red O staining showed that fenofibrate treatment reduced HFD-induced neutral lipid accumulation mainly in the glomeruli (Figure 2a). Consistent with this result, fenofibrate significantly attenuated HFD-induced increase in renal triglyceride content (Figure 2b). Immunohistochemical analysis of 4-hydroxynonenal-modified proteins, a marker of lipid peroxidation, showed that fenofibrate treatment reduced 4-hydroxynonenal accumulation in glomeruli (Figure 2c). Similarly, in the renal cortex of HFD-fed mice, fenofibrate treatment significantly reduced the content of malondialdehyde, which reflects the degree of lipid peroxidation (Figure 2d). In addition, fenofibrate treatment significantly increased the expression levels of lipolytic genes, such as acyl-CoA oxidase (ACO), medium-chain acyl-CoA dehydrogenase, and carnitine palmitoyltransferase-1 (CPT-1), in the kidney of HFD-fed mice (Table 2). These changes in the expression levels of ACO and CPT-1 were confirmed by western blot analysis (Figure 2e, f and g). Sterol regulatory element-binding transcription factor-1c (SREBP-1c) is a transcriptional factor regulating gene expression of lipogenic enzymes such as acetyl-CoA carboxylase. Protein expression of the active form of SREBP-1c tended to increase in the kidney of HFD-fed mice, which was not affected by fenofibrate treatment (Figure 2e and h). Accordingly, renal protein and mRNA expression of acetyl-CoA carboxylase-α in four groups of mice showed a similar tendency to the

Table 1 | Characteristics and results of IPITT at the end of 12-week experimental period in HFD model

	LFD		HFD	
	Control	Fenofibrate	Control	Fenofibrate
Characteristics				
Body weight (g)	30.2 ± 0.46[b]	26.2 ± 0.50[b]	45.6 ± 1.09[a]	38.5 ± 1.31[a,b]
Fasting blood glucose (mg/dl)	114.1 ± 6.15[b]	114.8 ± 5.52[b]	197.4 ± 16.35[a]	124.6 ± 7.55[b]
Plasma triglyceride (mg/dl)	62.0 ± 7.8	44.4 ± 2.6[b]	81.8 ± 5.9	51.8 ± 3.7[b]
Plasma cholesterol (mg/dl)	113.0 ± 10.3[b]	119.2 ± 3.4[b]	169.9 ± 7.6[a]	156.5 ± 16.4[a]
Plasma FFA (mEq/l)	1.02 ± 0.11	0.79 ± 0.10	0.70 ± 0.04[a]	0.56 ± 0.02[a]
Hemoglobin A1c (%)	3.1 ± 0.12[b]	3.3 ± 0.07[b]	3.9 ± 0.08[a]	3.7 ± 0.10
Plasma insulin (ng/ml)	0.32 ± 0.16[b]	0.18 ± 0.06[b]	1.47 ± 0.38[a]	0.48 ± 0.12[b]
Systolic blood pressure (mm Hg)	106.4 ± 4.9	94.6 ± 7.5	113.5 ± 4.6	109.1 ± 2.3
Food intake (kcal/day)	11.2 ± 0.69[b]	10.8 ± 0.13[b]	15.1 ± 0.42[a]	15.6 ± 0.89[a]
Urinary albumin excretion (μg/day)	18.8 ± 4.8[b]	6.0 ± 1.0[b]	50.4 ± 10.0[a]	20.2 ± 4.6[b]
IPITT				
Glucose level at basal (mg/dl)	142.5 ± 9.5[b]	127.3 ± 6.3[b]	261.5 ± 31.4[a]	118.0 ± 10.5[b]
Glucose level at 15 min (mg/dl)	80.5 ± 2.6[b]	75.8 ± 7.4[b]	260.0 ± 40.3[a]	71.0 ± 6.6[b]
Glucose level at 30 min (mg/dl)	63.8 ± 5.0[b]	63.5 ± 5.7[b]	221.3 ± 37.3[a]	55.8 ± 5.4[b]
Glucose level at 60 min (mg/dl)	55.8 ± 11.1[b]	69.8 ± 7.0[b]	206.8 ± 30.3[a]	60.8 ± 7.2[b]

Abbreviations: FFA, free fatty acid; HFD, high-fat diet; IPITT, intraperitoneal insulin tolerance test; LFD, low-fat diet.
Data are mean ± s.e.m.; n=8 (except for food intake and IPITT) in each group and n=4 (food intake and IPITT) in each group.
[a]$P<0.05$ versus mice fed LFD and [b]$P<0.05$ versus mice fed HFD.

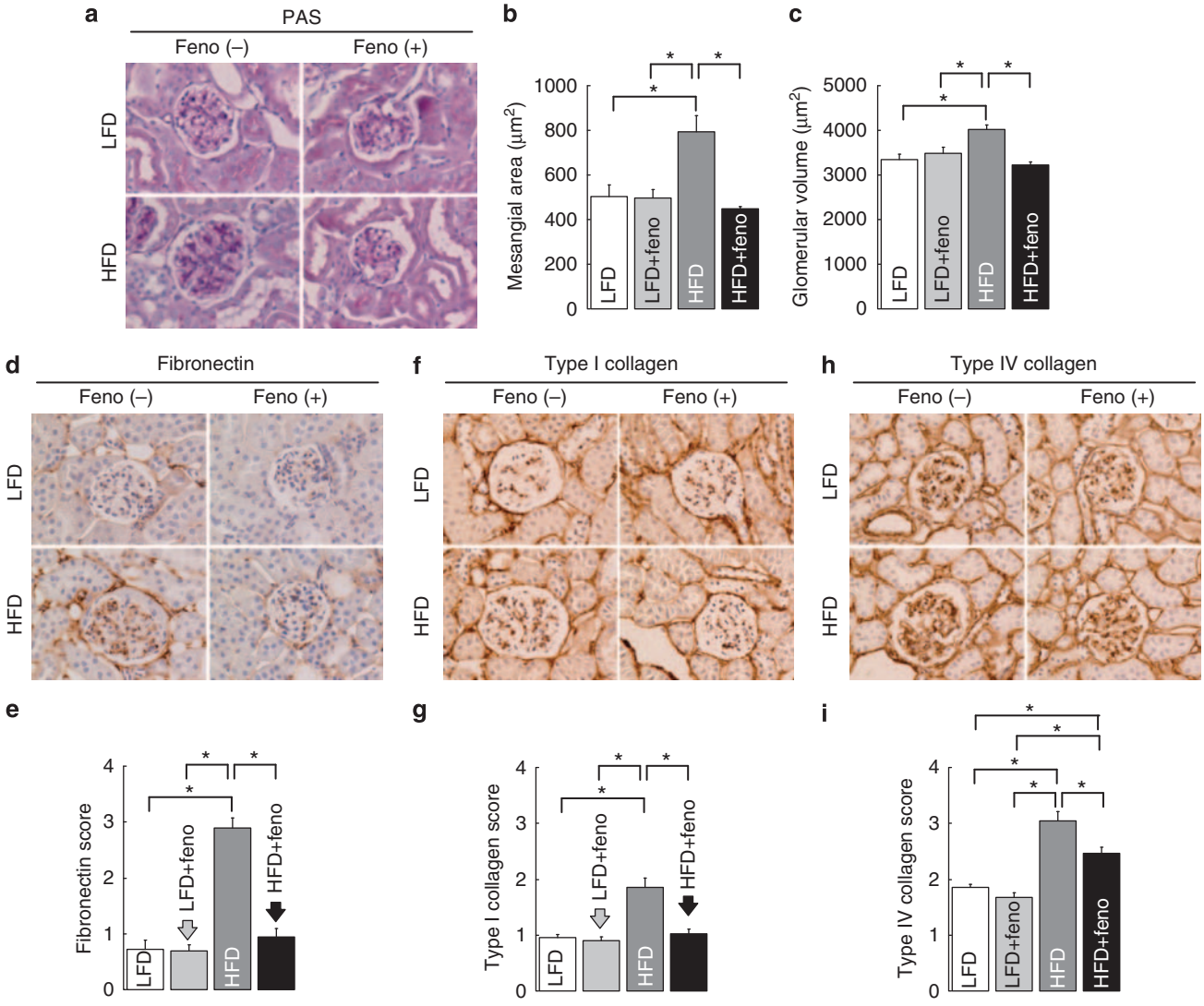

Figure 1 | Fenofibrate prevents HFD-induced glomerular injury. (**a**) Representative photomicrographs of periodic acid-Schiff (PAS)-stained glomeruli in kidney sections in LFD-fed and HFD-fed mice with or without fenofibrate (LFD, LFD + feno, HFD, and HFD + feno). Magnification × 400. (**b**, **c**) Quantitative analysis of mesangial area (**b**) and glomerular volume (**c**) in 20 glomeruli per mouse. Data are mean ± s.e.m. of eight mice in each group. (**d**) Representative photomicrographs of glomeruli in kidney sections immunostained for fibronectin in each group. Magnification × 400. (**e**) Quantitative analysis of fibronectin score in 20 glomeruli per mouse. Data are mean ± s.e.m. of four mice in each group. (**f**) Representative photomicrographs of glomeruli in kidney sections immunostained for type I collagen in each group. Magnification × 400. (**g**) Quantitative analysis of type I collagen score in 20 glomeruli per mouse. Data are mean ± s.e.m. of four mice in each group. (**h**) Representative photomicrographs of glomeruli in kidney sections immunostained for type IV collagen in each group. Magnification × 400. (**i**) Quantitative analysis of type IV collagen score in 20 glomeruli per mouse. Data are mean ± s.e.m. of four mice in each group. *$P < 0.05$. feno, fenofibrate; HFD, high-fat diet; LFD, low-fat diet.

expression level of SREBP-1c (Figure 2e and i, Table 2). No significant difference in renal expression of another transcriptional regulator of lipogenesis, PPARγ, was observed in all groups (Table 2). Furthermore, fenofibrate significantly increased the mRNA expression levels of antioxidant genes, such as catalase, Cu/Zn-superoxide dismutase, and Mn-superoxide dismutase, in the renal cortex of HFD-fed mice (Table 2). Taken together, fenofibrate seems to attenuate albuminuria and glomerular fibrosis in HFD-fed obese mice, accompanied by enhancement of renal lipolysis and antioxidant defenses.

Fenofibrate has antifibrotic action and attenuates oxidative stress in cultured mesangial cells

We next investigated the mRNA expression of PAI-1 in cultured mesangial cells stimulated by palmitate, a saturated fatty acid, to determine the direct protective effect of fenofibrate on lipotoxicity-mediated glomerular injury. In mesangial cells, palmitate significantly increased the mRNA expression level of PAI-1 (Figure 3a). Pretreatment with fenofibrate significantly attenuated palmitate-induced overexpression of PAI-1 in a dose-dependent manner (Figure 3a). In addition, pretreatment with fenofibrate significantly

Table 2 | The mRNA expression levels in the renal cortex at the end of 12-week experimental period in HFD model

	LFD		HFD	
	Control	Fenofibrate	Control	Fenofibrate
Fibrosis				
Fibronectin	0.95 ± 0.12^{b}	1.36 ± 0.13	1.86 ± 0.33^{a}	0.98 ± 0.14^{b}
PAI-1	1.43 ± 0.19^{b}	0.88 ± 0.11^{b}	2.89 ± 0.39^{a}	1.00 ± 0.16^{b}
Lipolysis				
PPARα	0.96 ± 0.11	1.82 ± 0.34	1.12 ± 0.08	1.74 ± 0.15
ACO	1.11 ± 0.18	1.41 ± 0.12	0.58 ± 0.05	1.47 ± 0.32^{b}
MCAD	0.88 ± 0.10	$1.54 \pm 0.12^{a,b}$	0.58 ± 0.03	1.39 ± 0.20^{b}
CPT-1	1.02 ± 0.11	1.24 ± 0.07	0.87 ± 0.07	1.29 ± 0.10^{b}
Lipogenesis				
ACCα	1.29 ± 0.14	1.71 ± 0.23	1.79 ± 0.21	1.65 ± 0.10
PPARγ	0.72 ± 0.09	0.84 ± 0.08	0.88 ± 0.06	0.70 ± 0.11
Anti-oxidant				
Catalase	0.91 ± 0.08	0.92 ± 0.05	0.84 ± 0.06	$1.26 \pm 0.09^{a,b}$
Cu/Zn-SOD	0.92 ± 0.06	1.06 ± 0.08	0.80 ± 0.11	$1.89 \pm 0.20^{a,b}$
Mn-SOD	0.86 ± 0.04	1.19 ± 0.13	1.04 ± 0.06	$1.54 \pm 0.12^{a,b}$

Abbreviations: ACC, acetyl-CoA carboxylase; ACO, acyl-CoA oxidase; CPT-1, carnitine palmitoyltransferase-1; HFD, high-fat diet; LFD, low-fat diet; MCAD, medium-chain acyl-CoA dehydrogenase; PAI-1, plasminogen activator inhibitor-1; PPAR, peroxisome proliferator-activated receptor; SOD, superoxide dismutase.
Data are mean ± s.e.m.; $n=6$ in each group.
$^{a}P<0.05$ versus mice fed LFD and $^{b}P<0.05$ versus mice fed HFD.

increased the mRNA expression levels of ACO and CPT-1 in a dose-dependent manner, and tended to increase the mRNA expression level of medium-chain acyl-CoA dehydrogenase in palmitate-stimulated mesangial cells (Figure 3b–d). Furthermore, pretreatment with fenofibrate significantly reduced the production of reactive oxygen species (ROS) in palmitate-stimulated mesangial cells (Figure 3e).

Fenofibrate attenuates FFA-bound BSA-overload tubulointerstitial injury

To determine whether PPARα agonist has a protective role against tubulointerstitial lesion in proteinuric kidney disease, we examined the effect of fenofibrate on FFA-bound BSA-overload nephropathy model. Neither BSA overload nor fenofibrate treatment influenced the systemic parameters at the end of the experiment (Table 3). Fenofibrate treatment tended to reduce proteinuria in FFA-bound BSA-overloaded mice, although the effect was not significant (Table 3). Morphological analysis of the kidneys of FFA-bound BSA-overloaded mice showed tubular dilatation, tubular vacuolation, and detachment of proximal tubular cells from the tubular basement membrane and interstitial edema (Figure 4a and b). Furthermore, the deposition of fibronectin (Figure 4c and d), type I collagen (Figure 4e and f) and IV collagen (Figure 4g and h), and infiltration of macrophages in the interstitium (Figure 4i and j) were significantly increased in the FFA-bound BSA-overloaded mice. Fenofibrate treatment significantly attenuated these histological abnormalities in the FFA-bound BSA-overloaded mice (Figure 4a–j). Compatible with these morphological changes, FFA-bound BSA-overload-induced increases in the mRNA expression levels of fibronectin, PAI-1, and monocyte chemoattractant protein-1 (MCP-1), a marker of inflammation, in the kidney were significantly inhibited by fenofibrate treatment (Table 4). The renal mRNA expression level of PPARα was significantly decreased by FFA-bound BSA-overload, which was not affected by fenofibrate treatment (Table 4).

Fenofibrate enhances renal lipolysis and attenuates oxidative stress in FFA-bound BSA-overloaded mice

Immunohistochemical analysis showed that fenofibrate treatment attenuated the FFA-bound BSA-overload-induced increase in accumulation of 4-hydroxynonenal-modified proteins in the renal interstitium (Figure 5a). Similarly, increased renal malondialdehyde contents in FFA-bound BSA-overloaded mice were significantly reduced by fenofibrate treatment (Figure 5b). Fenofibrate treatment increased the mRNA expression levels of lipolytic enzymes such as ACO, medium-chain acyl-CoA dehydrogenase, and CPT-1 in the kidneys of both phosphate-buffered saline (PBS)-injected and FFA-bound BSA-overloaded mice (Table 4). These changes in the expression levels of ACO and CPT-1 were confirmed by western blot analysis (Figure 5c–e). As for the expression of renal lipogenic enzymes, significant changes in protein and mRNA expression of lipogenic genes, such as *SREBP-1c*, *acetyl-CoA carboxylase-α* and *PPARγ*, were not observed in the kidneys of all groups (Figure 5c, f and g, Table 4). Furthermore, fenofibrate treatment did not affect the mRNA expression levels of antioxidant genes in FFA-bound BSA-overloaded mice (Table 4). These results indicate that fenofibrate attenuates tubulointerstitial fibrosis and inflammation, with enhancement of renal lipolysis in the FFA-bound BSA-overloaded mice.

Fenofibrate has antifibrotic and anti-inflammatory effects, and attenuates oxidative stress in cultured proximal tubular cells

To examine the direct renoprotective effect of fenofibrate on tubulointerstitial inflammation and fibrosis, we examined the mRNA expression levels of MCP-1 and PAI-1 in palmitate-stimulated cultured murine proximal tubular cells. Palmitate stimulation significantly increased the mRNA expression levels of MCP-1 and PAI-1 (Figure 6a and b). Pretreatment of fenofibrate significantly attenuated the increased mRNA expression levels of MCP-1 and PAI-1 (Figure 6a and b). Similar to the results for mesangial cells, pretreatment with fenofibrate significantly increased the mRNA expression levels of ACO, medium-chain acyl-CoA dehydrogenase, and CPT-1 in palmitate-stimulated proximal tubular cells (Figure 6c–e). Furthermore, pretreatment with fenofibrate significantly reduced ROS production in palmitate-stimulated proximal tubular cells (Figure 6f).

DISCUSSION

The present study showed that fenofibrate, a PPARα agonist, attenuated glomerular injury in HFD-fed obese mice and

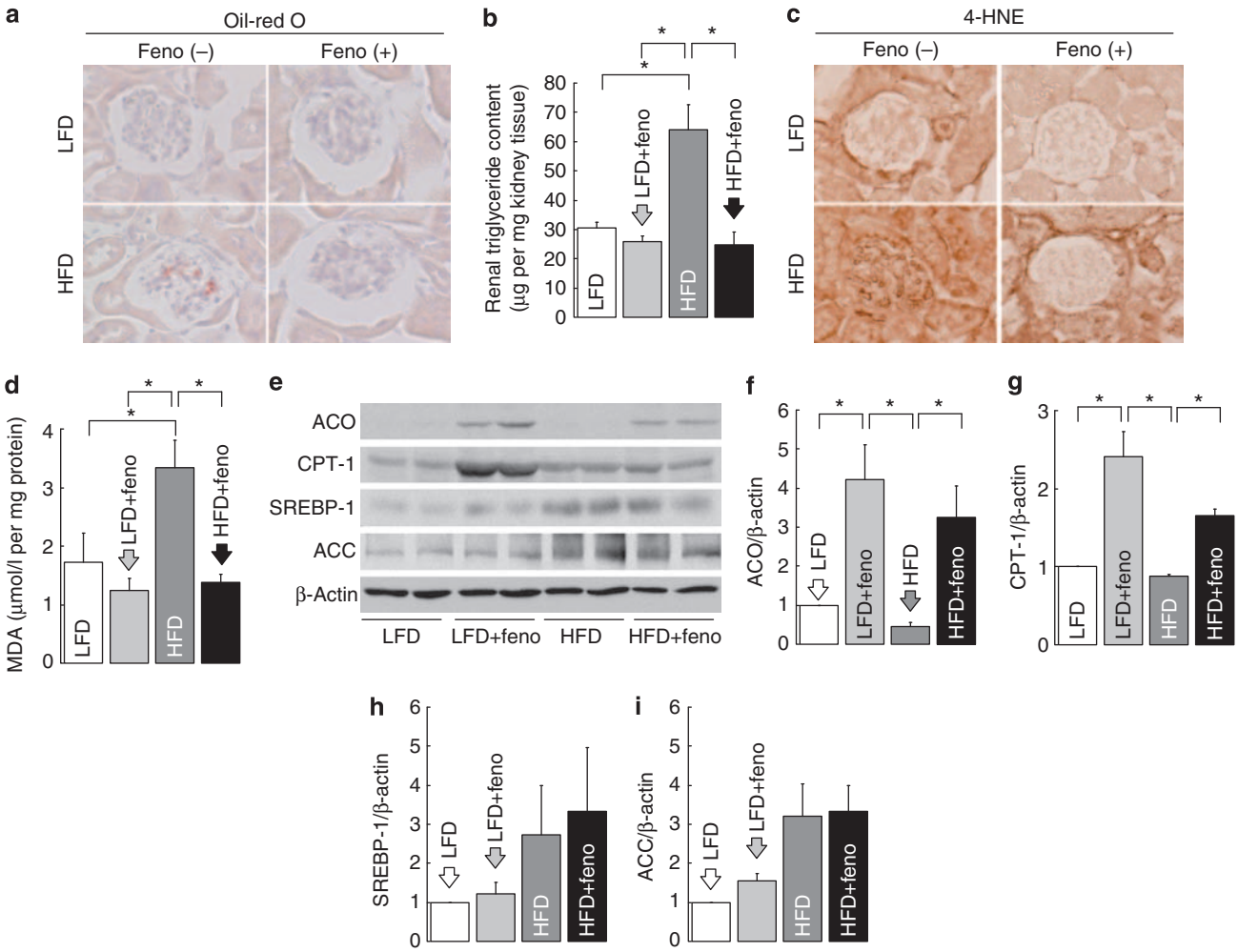

Figure 2 | Fenofibrate prevents HFD-induced lipid accumulation and oxidative stress in the glomeruli. (**a**) Representative photomicrographs of oil-red O-stained glomeruli in kidney sections in LFD-fed and HFD-fed mice with or without fenofibrate. Magnification $\times 400$. (**b**) Triglyceride contents in the renal cortex of mice in each group. Data are mean ± s.e.m. of 4–7 mice in each group. (**c**) Representative photomicrographs of glomeruli in kidney sections immunostained for 4-HNE in each group. Magnification $\times 400$. (**d**) MDA contents in the renal cortex in each group. Data are mean ± s.e.m. of six mice in each group. (**e**) Representative immunoblots of ACO, CPT-1, SREBP-1, and ACC in protein extracted from the renal cortex of mice of each group. β-Actin was loaded as an internal control. (**f**) Quantitative analysis of ACO protein expression. (**g**) Quantitative analysis of CPT-1 protein expression. (**h**) Quantitative analysis of SREBP-1 protein expression. (**i**) Quantitative analysis of ACC protein expression. Data are mean ± s.e.m. of six mice in each group. $^*P<0.05$. ACC, acetyl-CoA carboxylase; ACO, acyl-CoA oxidase; CPT-1, carnitine palmitoyltransferase-1; feno, fenofibrate; HFD, high-fat diet; 4-HNE, 4-hydroxynonenal; LFD, low-fat diet; MDA, malondialdehyde; SREBP-1, sterol regulatory element-binding protein-1.

tubulointerstitial injury in FFA-bound BSA-overload nephropathy mice. These renoprotective effects of fenofibrate were accompanied by enhancement of renal lipolysis, which consequently prevented lipid accumulation, oxidative stress, fibrosis, and inflammation. These results highlight the importance of PPARα-mediated enhancement of renal lipolysis as novel therapeutic strategy for prevention of both initiation and progression of CKD.

We have previously reported that mice with HFD-induced obesity exhibit renal lesions similar to CKD in patients with metabolic syndrome.[6,16] The present study provided the first evidence for the renobeneficial effects of fenofibrate against albuminuria and glomerular lesions in HFD-fed mice. PPARα is expressed in several organs, such as liver and skeletal muscle. PPARα agonists induce lipolysis in these metabolic organs and subsequently attenuate insulin resistance in diet-induced obese model[17] and type 2 diabetic db/db mice,[18] which was confirmed in our study. The present study showed for the first time that fenofibrate could enhance renal lipolysis as well as these metabolic organs. Furthermore, recent reports showed that fenofibrate attenuated renal injuries in spontaneously hypertensive rats fed a HFD[19] and type 2 diabetic db/db mice,[20] although the mechanisms of the renoprotective effects of fenofibrate in these models were not determined. As renal lipotoxicity is involved in the pathogenesis of renal injury in these models,[7,19] and based on our results, amelioration of intrarenal lipotoxicity with enhancement of renal lipolysis could explain the mechanism

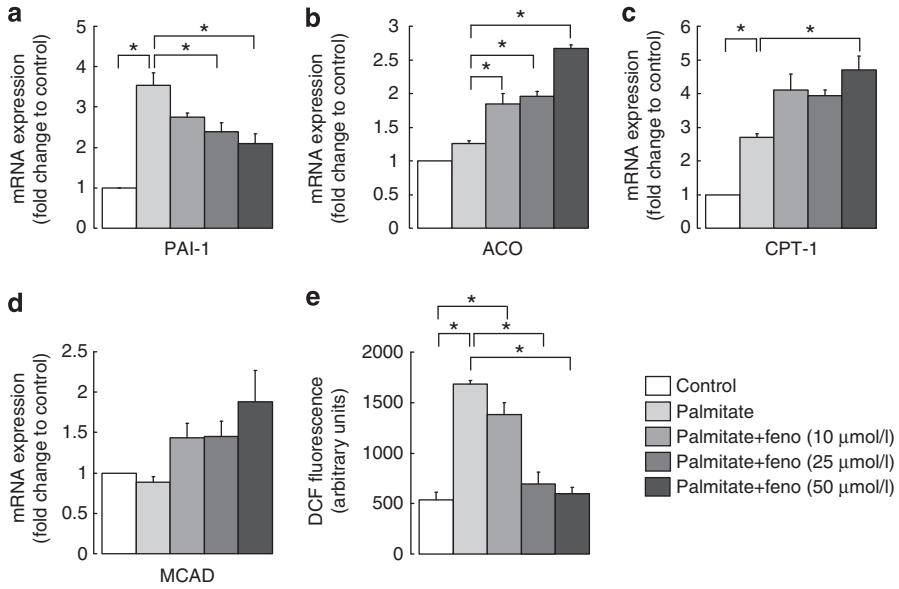

Figure 3 | Fenofibrate has an antifibrotic effect, enhances the expression of lipolytic enzymes, and reduces reactive oxygen species (ROS) in palmitate-stimulated cultured mesangial cells. (**a**) Quantification of PAI-1 mRNA expression in cultured mesangial cells stimulated by palmitate with or without pretreatment of fenofibrate at the indicated concentration (control, palmitate, palmitate + feno10, palmitate + feno25, and palmitate + feno50). Results are expressed as fold change relative to the mRNA of control. Data are mean ± s.e.m. (**b**–**d**) The mRNA expression levels of ACO (**b**), CPT-1 (**c**), and MCAD (**d**) in each group of mesangial cells. Data are mean ± s.e.m. (**e**) Intracellular production of ROS from mesangial cells in each group. The results are expressed in arbitrary units. Data are mean ± s.e.m. *$P<0.05$. ACO, acyl-CoA oxidase; CPT-1, carnitine palmitoyltransferase-1; DCF, 2.7-dichlorodihydrofluorescein; feno, fenofibrate; MCAD, medium-chain acyl-CoA dehydrogenase; PAI-1, plasminogen activator inhibitor-1.

Table 3 | Characteristics at the end of experimental period in mice with FFA-bound BSA-overload model

	PBS		FFA-bound BSA	
	Control	Fenofibrate	Control	Fenofibrate
Body weight (g)	22.9 ± 0.52	22.5 ± 0.42	23.7 ± 0.25	23.4 ± 0.58
Blood glucose (mg/dl)	159.2 ± 9.0	142.0 ± 11.3	141.0 ± 8.1	137.5 ± 11.3
Plasma insulin (ng/ml)	0.96 ± 0.38	0.92 ± 0.39	1.11 ± 0.28	1.03 ± 0.34
Urinary protein excretion (mg/day)	3.86 ± 0.67	2.95 ± 0.32	6.92 ± 1.51	3.79 ± 0.40

Abbreviations: BSA, bovine serum albumin; FFA, free fatty acid; PBS, phosphate-buffered saline.
Data are mean ± s.e.m.; n=5 in each group.

underlying fenofibrate-mediated renoprotective effects in these models.

In proteinuric kidney disease regardless of the metabolic disorder, tubulointerstitial damage, including fibrosis, proximal tubular cell damage, and inflammation, is closely associated with renal prognosis.[21] The increased reabsorption of FFA-bound albumin by proximal tubular cells has been confirmed as the pathogenic process responsible for tubulointerstitial damage in a FFA-bound BSA-overload nephropathy mouse model.[9,10] FFA-bound BSA overload resulted in severer tubular damage in *PPARα*-knockout[22] and *interleukin-18 receptor*-knockout mice.[23] However, no study has so far reported an effective therapeutic approach against this type of renal injury. We showed here that treatment with PPARα agonist, fenofibrate, improved tubulointerstitial injury, with enhancement of lipolysis and reduction of fibrosis, inflammation, and oxidative stress, suggesting that activation of endogenous level of PPARα seems to have a protective role against tubulointerstitial injury in proteinuric kidney disease by mediating renal lipid homeostasis.

Overexpression of lipogenic enzymes[24] and/or underexpression of lipolytic enzymes[25] in local tissues are reported to be one cause of lipid accumulation and subsequent tissue damage including renal injury. Thus, regulation of enzyme expression associated with lipid metabolism may be a suitable strategy against lipotoxicity-associated tissue dysfunction. Several reports suggested that PPARα agonists enhance lipolysis through upregulation of lipolytic enzymes, and thus improve lipotoxicity-mediated tissue damage in the liver and skeletal muscle.[17,26] In the present study, we confirmed that fenofibrate upregulated the expressions of lipolytic enzymes in the kidney, although it did not affect the expression levels of lipogenic enzymes. These results suggest that fenofibrate-mediated renal lipolysis with overexpression of lipolytic enzymes contributes to the improvement in renal lipotoxicity.

Lipid-mediated oxidative stress is considered to induce inflammation and fibrosis in the kidney. Accordingly, amelioration of lipotoxicity-induced renal oxidative stress

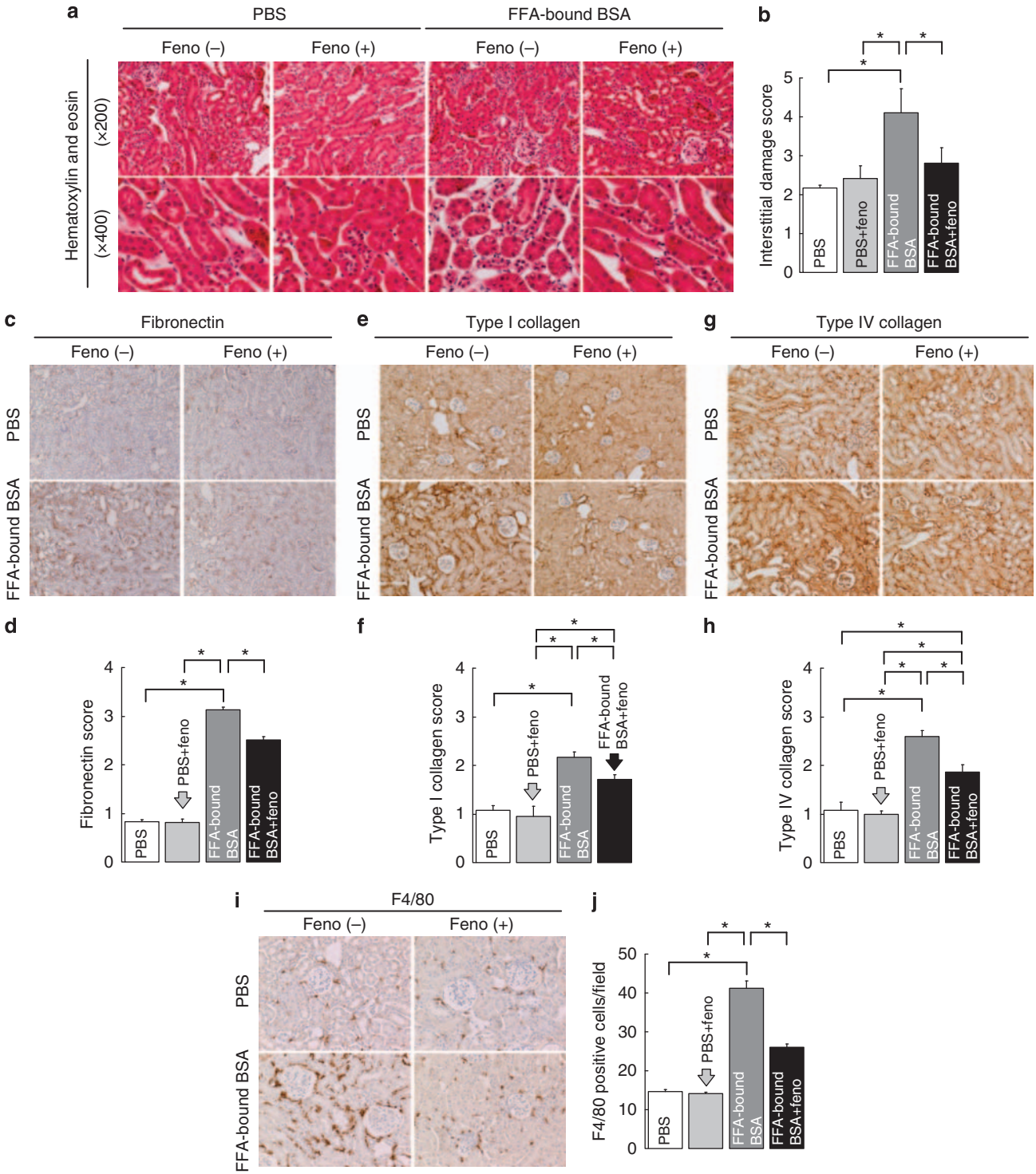

Figure 4 | Fenofibrate prevents free fatty acid (FFA)-bound bovine serum albumin (BSA)-induced interstitial lesion. (**a**) Representative photomicrographs of hematoxylin and eosin-stained kidney sections in PBS-injected and FFA-bound BSA-injected mice with or without fenofibrate (PBS, PBS + feno, FFA-bound BSA, and FFA-bound BSA + feno). Magnifications × 200 and × 400. (**b**) Quantitative analysis of interstitial damage score from 20 random fields per mouse. Data are mean ± s.e.m. of four mice in each group. (**c**) Representative photomicrographs of kidney sections immunostained for fibronectin in each group. Magnification × 100. (**d**) Quantitative analysis of fibronectin score from 20 random fields per mouse. Data are mean ± s.e.m. of four mice in each group. (**e**) Representative photomicrographs of kidney sections immunostained for type I collagen in each group. Magnification × 200. (**f**) Quantitative analysis of type I collagen score from 20 random fields per mouse. Data are mean ± s.e.m. of four mice in each group. (**g**) Representative photomicrographs of kidney sections immunostained for type IV collagen in each group. Magnification × 200. (**h**) Quantitative analysis of type IV collagen score from 20 random fields per mouse. Data are mean ± s.e.m. of four mice in each group. (**i**) Representative photomicrographs of kidney sections immunostained for F4/80 in each group. Magnification × 200. (**j**) Quantitative analysis of F4/80-positive cells from 20 random fields per mouse. Data are mean ± s.e.m. of four mice in each group. *$P < 0.05$. feno, fenofibrate; PBS, phosphate-buffered saline.

Table 4 | The mRNA expression levels in the kidney at the end of experimental period in mice with FFA-bound BSA-overload model

	PBS		FFA-bound BSA	
	Control	Fenofibrate	Control	Fenofibrate
Fibrosis and inflammation				
Fibronectin	1.04 ± 0.18^{b}	0.71 ± 0.03^{b}	1.62 ± 0.13^{a}	0.88 ± 0.07^{b}
PAI-1	0.61 ± 0.11^{b}	0.72 ± 0.20^{b}	1.53 ± 0.13^{a}	0.71 ± 0.07^{b}
MCP-1	0.55 ± 0.13^{b}	0.31 ± 0.03^{b}	1.50 ± 0.24^{a}	0.62 ± 0.12^{b}
Lipolysis				
PPARα	1.61 ± 0.26	1.85 ± 0.10^{b}	0.87 ± 0.10^{a}	1.14 ± 0.171
ACO	1.20 ± 0.16	1.71 ± 0.21	1.06 ± 0.15	$3.06 \pm 0.57^{a,b}$
MCAD	1.16 ± 0.16	1.25 ± 0.06	0.85 ± 0.09	$1.73 \pm 0.16^{a,b}$
CPT-1	1.35 ± 0.14	1.32 ± 0.13	0.96 ± 0.18	2.01 ± 0.30^{b}
Lipogenesis				
ACCα	0.75 ± 0.13	0.66 ± 0.07	1.27 ± 0.24	0.87 ± 0.14
PPARγ	0.72 ± 0.09	0.84 ± 0.08	0.88 ± 0.06	0.70 ± 0.11
Anti-oxidant				
Catalase	1.22 ± 0.13	0.97 ± 0.03	0.82 ± 0.04^{a}	0.76 ± 0.06^{a}
Cu/Zn-SOD	1.00 ± 0.02	1.27 ± 0.24	1.35 ± 0.31	1.01 ± 0.10
Mn-SOD	0.99 ± 0.11	0.99 ± 0.08	1.01 ± 0.16	1.00 ± 0.13

Abbreviations: ACC, acetyl-CoA carboxylase; ACO, acyl-CoA oxidase; BSA, bovine serum albumin; CPT-1, carnitine palmitoyltransferase-1; FFA, free fatty acid; MCP-1, monocyte chemoattractant protein-1; MCAD, medium-chain acyl-CoA dehydrogenase; PAI-1, plasminogen activator inhibitor-1; PBS, phosphate-buffered saline; PPAR, peroxisome proliferator-activated receptor; SOD, superoxide dismutase.
Data are mean ± s.e.m.; n=6 in each group.
$^{a}P<0.05$ versus PBS and $^{b}P<0.05$ versus FFA-bound BSA.

seems a conceivable therapy in CKD. In our *in vivo* study, fenofibrate ameliorated lipotoxicity-associated ROS accumulation in the kidneys of both HFD-fed obese mice and FFA-bound BSA-overload nephropathy mice. Generally, ROS accumulation occurs by an imbalance between ROS production and antioxidant defenses. Also, PPARα positively regulates the expression of genes associated with antioxidant in addition to those involved in lipolysis.[27] The present study showed that fenofibrate increased renal expression levels of lipolytic genes in both animal experimental models. In contrast, it increased the expression of antioxidant enzymes only in the kidney of HFD-fed mice, but not in FFA-bound BSA-overloaded mice. Based on these findings, the enhancement of renal lipolysis is more important for fenofibrate-mediated reduction of ROS in both mouse experimental models, although the strengthened antioxidant defenses may partially contribute to fenofibrate-mediated renoprotection in HFD model.

Our present study showed that FFA-bound BSA overload decreased PPARα expression in the kidney. In this regard, the previous study reported that FFA-bound BSA-overload caused severe tubular damage in *PPARα*-deficient mice.[22] These findings suggest that the decrease in renal PPARα expression might contribute to the pathogenesis of FFA-bound BSA-overload nephropathy. As for the role of endogenous PPARα expression on glomerular injury, until recently, there have been no reports showing the effect of *PPARα* deficiency on glomerular injury associated with metabolic disease. Based on the results from several previous studies, *PPARα*-knockout mice do not develop obesity and show hypoglycemia, even under a HFD.[28] Also, HFD-induced glomerular injury largely depends on systemic metabolic abnormality, such as obesity and insulin resistance.[6] Thus, systemic *PPARα*-knockout mouse would not be a suitable mouse model to conclude the exact role of renal *PPARα* deficiency in glomerular injury associated with metabolic disease. The experimental study using glomerular cell-specific *PPARα*-knockout mouse may prove it, although this type of mice model is not available now.

Interestingly, a recent clinical study showed the effective therapeutic potency of fenofibrate in diabetic nephropathy.[29] The Fenofibrate Intervention and Event Lowering in Diabetes (FIELD) study showed that fenofibrate prevented the initiation and progression of albuminuria in patients with type 2 diabetes mellitus.[29] Consistent with this result, our results suggest that enhancement of renal lipolysis may be involved in the mechanism underlying the renoprotective effect of fenofibrate seen in the FIELD study.

In conclusion, our study demonstrated that fenofibrate ameliorated the development of both glomerular lesion in HFD-fed mice and tubulointerstitial lesion in FFA-bound BSA-overload nephropathy mice, with enhancement of renal lipolysis. These results provide evidence that pharmacological activation of PPARα could be a therapeutically suitable strategy against glomerular and tubulointerstitial lesions in CKD.

MATERIALS AND METHODS

Animal models

All procedures were performed in accordance with the guidelines of the Research Center for Animal Life Science of Shiga University of Medical Science.

HFD-induced renal injury model. Five-week-old male C57BL/6 mice were purchased from CLEA Japan (Tokyo, Japan), and housed in cages and maintained on a 12-h light/12-h dark cycle. A low-fat diet (LFD: 10% of total calories from fat) and a HFD (60% of total calories from fat) were purchased from Research Diets (New Brunswick, NJ). After 2 weeks of acclimatization, 7-week-old mice were divided into four groups: LFD, LFD + fenofibrate, HFD, and HFD + fenofibrate group (n = 13, 9, 13 and 8, respectively), and received LFD, HFD, LFD, or HFD, respectively, supplemented with fenofibrate (0.05% wt/wt)[30,31] (Teijin Pharma, Tokyo, Japan) for 12 weeks. At the end of the 12-week experimental period, body weight, blood glucose level, and systolic blood pressure[16] were measured, and an intraperitoneal insulin tolerance test[6] was performed. Mice were placed in metabolic balance cages for 24-h urine collection. After the 24-h urine collection, mice were anesthetized by intraperitoneal injection of pentobarbital sodium (50 mg/kg body weight), and then blood was drawn for biochemical assay. The kidneys were removed as previous.[16]

FFA-bound BSA-induced renal injury model. Seven-week-old male C57BL/6 mice were divided into four groups: PBS, PBS + fenofibrate, FFA-bound BSA, and FFA-bound BSA + fenofibrate group (n = 6, 6, 9, and 6, respectively). Mice were fed either a standard diet or the same diet supplemented with fenofibrate (0.05% wt/wt). At 3 days after the assignation to either diet, the mice of each group were given consecutive daily intraperitoneal bolus

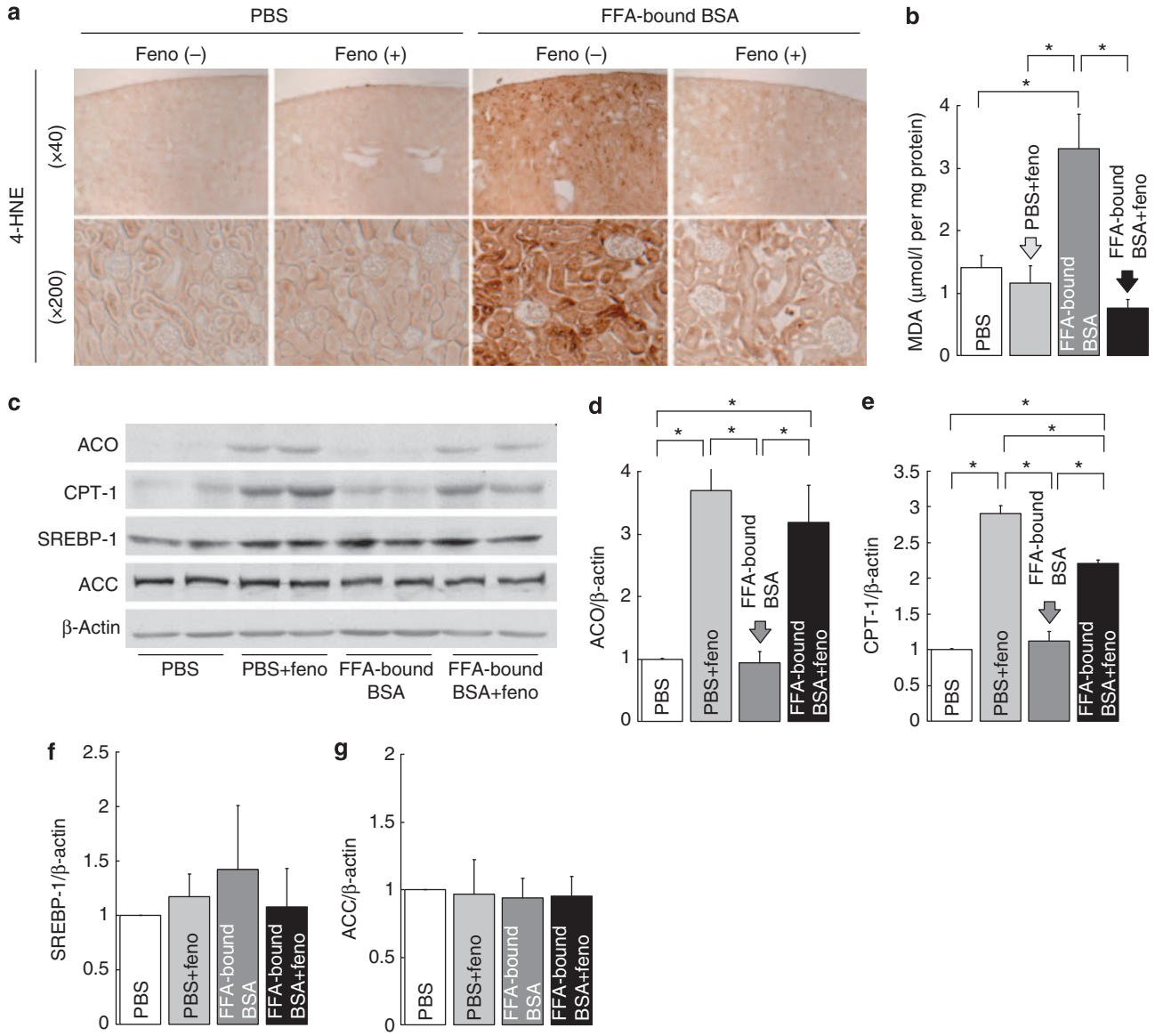

Figure 5 | Fenofibrate prevents the increase of oxidative stress in the kidney of free fatty acid (FFA)-bound bovine serum albumin (BSA)-overload nephropathy. (**a**) Representative photomicrographs of kidney sections immunostained for 4-HNE in PBS-injected and FFA-bound BSA-injected mice with or without fenofibrate. Magnifications × 40 and × 200. (**b**) MDA contents in the kidney in each group. Data are mean ± s.e.m. of six mice in each group. (**c**) Representative immunoblots of ACO, CPT-1, SREBP-1, and ACC in protein extracted from kidney of mice in each group. β-Actin was loaded as an internal control. (**d**) Quantitative analysis of ACO protein expression. (**e**) Quantitative analysis of CPT-1 protein expression. (**f**) Quantitative analysis of SREBP-1 protein expression. (**g**) Quantitative analysis of ACC protein expression. Data are mean ± s.e.m. of six mice in each group. *$P < 0.05$. ACC, acetyl-CoA carboxylase; ACO, acyl-CoA oxidase; CPT-1, carnitine palmitoyltransferase-1; feno, fenofibrate; 4-HNE, 4-hydroxynonenal; MDA, malondialdehyde; PBS, phosphate-buffered saline; SREBP-1, sterol regulatory element-binding protein-1.

injection of either 0.3 g/30 g body weight FFA-bound BSA (Sigma Chemical, St Louis, MO) diluted in sterile PBS or equal volume of sterile PBS as control for 11 days. After the injection of BSA or PBS on day 11, urine was collected over 24 h. At the end of the experiment, mice were anesthetized and perfused as reported previously.[16]

Blood and urine analysis

Serum triglycerides and total cholesterol were measured using L type TG H kit and Cholesterol E-test kit, respectively (Wako Chemicals, Osaka, Japan). Serum FFA level was determined using nonesterified fatty acid C-test kit (Wako Chemicals). Hemoglobin A1c was measured using the DCA 2000 analyzer (Siemens Medical Solutions Diagnostics, Tokyo, Japan). Plasma insulin was measured using an ELISA kit (Morinaga Institute of Biological Science, Tokyo, Japan). Urinary albumin and urinary protein concentration were measured with an ELISA kit (Exocell, Philadelphia, PA) and Bradford method, respectively.

Histological and immunohistochemical analyses

Fixed kidneys embedded in paraffin were sectioned (3-μm thickness). Semiquantitative histological analysis for glomerular lesions was performed using periodic acid-Schiff-stained sections, as

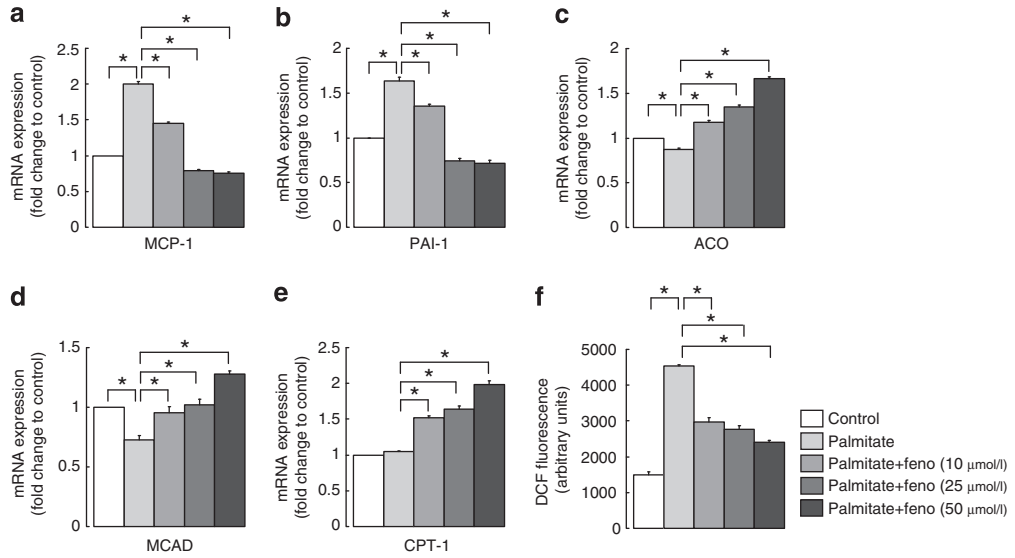

Figure 6 | Fenofibrate has antifibrotic and anti-inflammatory effects, enhances lipolytic enzymes, and reduces reactive oxygen species (ROS) in palmitate-stimulated cultured proximal tubular cells. (**a**, **b**) Quantification of MCP-1 (**a**) and PAI-1 (**b**) mRNA expression levels in cultured proximal tubular cells stimulated by palmitate with or without pretreatment of fenofibrate at the indicated concentration (control, palmitate, palmitate + feno10, palmitate + feno25, and palmitate + feno50). Results are expressed as fold change relative to the mRNA of the control. Data are mean ± s.e.m. (**c**–**e**) The mRNA expression levels of ACO (**c**), MCAD (**d**), and CPT-1 (**e**) in each group of proximal tubular cells. Data are mean ± s.e.m. (**f**) Intracellular production of ROS from proximal tubular cells in each group. Results are expressed in arbitrary units. Data are mean ± s.e.m. *$P < 0.05$. ACO, acyl-CoA oxidase; CPT-1, carnitine palmitoyltransferase-1; DCF, 2.7-dichlorodihydrofluorescein; feno, fenofibrate; MCP-1, monocyte chemoattractant protein-1; MCAD, medium-chain acyl-CoA dehydrogenase; PAI-1, plasminogen activator inhibitor-1.

reported previously.[16] Semiquantitative histological analysis for interstitial lesion was performed using hematoxylin and eosin-stained sections as reported previously.[32]

Immunohistochemical staining was performed with F4/80-specific monoclonal anti-rat antibody (Serotec, Oxford, UK), fibronectin-specific polyclonal anti-rabbit antibody (Chemicon International, Temecula, CA), type I collagen-specific polyclonal anti-goat antibody (Southern Biotech, Birmingham, AL), type IV collagen-specific polyclonal anti-rabbit antibody (Millipore, Billerica, MA), and 4-hydroxy-2-nonenal monoclonal anti-mouse antibody (JaICA, Shizuoka, Japan). For evaluation of immunostaining for fibronectin, the percentages of area stained for fibronectin were graded as follows: grade 0, staining absent to 5%; grade 1, 5–25%; grade 2, 25–50%; grade 3, 50–75%; and grade 4, >75%.[6] For evaluation of immunostaining for type I collagen and type IV collagen, changes in the extent and the intensity of staining were rated using the following grades: grade 0, no; grade 1, minor; grade 2, moderate; grade 3, severe; and grade 4, most severe changes. For evaluation of immunostaining for F4/80, F4/80-positive cells were counted in 20 randomly selected areas.[16] Accumulation of neutral lipids was evaluated using 4-μm-thick oil-red O-stained frozen sections.[6]

Lipid extraction and measurement of triglyceride concentration

Total lipid was extracted from the renal cortex in HFD model and from the kidney in BSA model by the method of Bligh and Dyer.[33] Triglyceride contents were determined as described previously.[6]

Measurement of lipid peroxidation

The extent of lipid peroxidation was measured by the thiobarbituric acid reactive substances assay using malondialdehyde assay kit (JaICA). The malondialdehyde concentration was normalized to the protein concentration.

Protein extraction and western blot analysis

The renal cortex in HFD model and the kidney in BSA model were homogenized in an ice-cold lysis buffer containing 150 mmol/l NaCl, 50 mmol/l Tris-HCl (pH 8.0), 0.1% SDS, 1% Nonidet P-40, and protease inhibitor cocktail (Boehringer Mannheim, Lewes, UK). These samples were resolved by 10% SDS-polyacrylamide gel electrophoresis and transferred to polyvinylidene fluoride membranes (Immobilon, Bedford, MA). The membranes were incubated with ACO-specific polyclonal anti-rabbit antibody (Abcam, Cambridge, UK), CPT-1-specific polyclonal anti-goat antibody (Santa Cruz Biotechnology, Santa Cruz, CA), SREBP-1-specific monoclonal anti-mouse antibody (Thermo Fisher Scientific, Waltham, MA), and acetyl-CoA carboxylase-specific monoclonal anti-rabbit antibody (Cell Signaling Technology, Beverly, MA), washed and incubated with horseradish peroxidase-coupled secondary antibodies (Amersham, Buckinghamshire, UK). The blots were visualized by using an enhanced chemiluminescence detection system (Perkin Elmer Life Science, Boston, MA).

Mouse mesangial and proximal tubular cells

SV40-transformed murine mesangial cell line and murine proximal tubular cell line were cultured as described previously.[34,35] First, we confirmed that the dose of fenofibrate we used in this experiment was not cytotoxic in both cells using AlamarBlue Assay (Alamar Bioscience, Sacramento, CA; data not shown). Next, we confirmed that among several FFAs, including palmitate (a saturated fatty acid), oleate (a monounsaturated fatty acid), eicosapentaenoic acid (an ω-3 polyunsaturated fatty acid), and linoleate (an ω-6 polyunsaturated fatty acid), only palmitate increased the mRNA

Table 5 | Sequences of primers used for real-time PCR

Primer	Forward	Reverse
β-Actin	CGTGCGTGACATCAAAGAGAA	TGGATGCCACAGGATTCCAT
Fibronectin	AGACCATACCTGCCGAATGTAG	GAGAGCTTCCTGTCCTGTAGAG
PAI-1	GGACACCCTCAGCATGTTCA	TCTGATGAGTTCAGCATCCAAGAT
MCP-1	GCCCCACTCACCTGCTGCTACT	CCTGCTGCTGGTGATCCTCTTGT
PPARα	ATGCCAGTACTGCCGTTTTC	CCGAATCTTTCAGGTCGTGT
ACO	GGCCAACTATGGTGGACATCA	ACCAATCTGGCTGCTGCACGAA
MCAD	TAATCGGTGAAGGAGCAGGTTT	GGCATACTTCGTGGCTTCGT
CPT-1	ACCACTGGCCGAATGTCAAG	AGCGAGTAGCGCATGGTCAT
ACCα	CCCAGCAGAATAAAGCTACTTTGG	TCCTTTTGTGCAACTAGGAACGT
PPARγ	CCAGAGTCTGCTGATCTGC	GCCACCTCTTTGCTCTGCTC
Catalase	GCCAGAAGAGAAACCCACAGA	ACAAGAAAGAAACCTGATGGAGAGA
Cu/Zn-SOD	AATGGTGGTCCATGAGAAACAAG	GCAATCCCAATCACTCCACA
Mn-SOD	CTTCAATAAGGAGCAAGGTCGC	CACACGTCAATCCCCAGC

Abbreviations: ACC, acetyl-CoA carboxylase; ACO, acyl-CoA oxidase; CPT-1, carnitine palmitoyltransferase-1; MCAD, medium-chain acyl-CoA dehydrogenase; MCP-1, monocyte chemoattractant protein-1; PAI-1, plasminogen activator inhibitor-1; PPAR, peroxisome proliferator-activated receptor; SOD, superoxide dismutase.

expression level of PAI-1 and MCP-1 in both cells (data not shown). Then, to evaluate the effect of fenofibrate on lipotoxicity-associated fibrosis and inflammation, subconfluent cultured cells were serum starved for 24 h in the presence or absence of fenofibrate (dissolved in dimethyl sulfoxide) at a final concentration of 10, 25, and 50 μmol/l, followed by stimulation with 200 μmol/l of palmitate (Sigma Chemical) in 8.0% BSA or same concentration of BSA, as control for 12 h.

RNA extraction and quantitative real-time PCR

Total RNA was isolated from the kidney or cultured renal cells, and cDNA was synthesized as described previously.[16] The iQSYBR Green Supermix (Bio-Rad Laboratories, Hercules, CA) was used for real-time PCR (ABI Prism TM 7500 Sequence Detection System; Perkin-Elmer Applied Biosystems, Foster City, CA). The expression levels of mRNAs were quantified using the standard curve method, as reported previously.[16] Analytical data were adjusted, with the expression level of mRNA of β-actin as an internal control. Primer sequences are described in Table 5.

Measurement of intracellular ROS

ROS generation was measured with fluoroprobe 2.7-dichlorodihydrofluorescein diacetate (Molecular Probes, Eugene, OR), which is taken up by the cell and converted by intracellular esterases to 2.7-dichlorodihydrofluorescein. ROS generation was evaluated as the fluorescence intensity (excitation wavelength 488 nm and emission wavelength 525 nm) of 2.7-dichlorodihydrofluorescein by an Infinite M200 microplate reader (Tecan Japan, Kanagawa, Japan) after 3 h of palmitate stimulation. The results of intracellular ROS generation are expressed in arbitrary units.

Statistical analysis

Results are expressed as mean ± s.e.m. Analysis of variance with subsequent Scheffe test was used to determine the significance of differences in multiple comparisons. A P-value <0.05 was considered statistically significant.

DISCLOSURE

All the authors declared no competing interests.

ACKNOWLEDGMENTS

We are grateful to Yuji Kamijo (Shinshu University School of Medicine, Nagano, Japan) for helpful suggestion on FFA-bound BSA-overload nephropathy mouse model. We also thank Makiko Sera (Shiga University of Medical Science, Shiga, Japan) and the Central Research Laboratory of Shiga University of Medical Science for the technical assistance. This work was supported by the JSPS KAKENHI (21591130) and Takeda Science Foundation (to KI).

REFERENCES

1. Go AS, Chertow GM, Fan D *et al.* Chronic kidney disease and the risks of death, cardiovascular events, and hospitalization. *N Engl J Med* 2004; **351**: 1296–1305.
2. Abrass CK. Cellular lipid metabolism and the role of lipids in progressive renal disease. *Am J Nephrol* 2004; **24**: 46–53.
3. Bagby SP. Obesity-initiated metabolic syndrome and the kidney: a recipe for chronic kidney disease? *J Am Soc Nephrol* 2004; **15**: 2775–2791.
4. Schaffer JE. Lipotoxicity: when tissues overeat. *Curr Opin Lipidol* 2003; **14**: 281–287.
5. Unger RH, Orci L. Diseases of liporegulation: new perspective on obesity and related disorders. *FASEB J* 2001; **15**: 312–321.
6. Kume S, Uzu T, Araki S *et al.* Role of altered renal lipid metabolism in the development of renal injury induced by a high-fat diet. *J Am Soc Nephrol* 2007; **18**: 2715–2723.
7. Wang Z, Jiang T, Li J *et al.* Regulation of renal lipid metabolism, lipid accumulation, and glomerulosclerosis in FVBdb/db mice with type 2 diabetes. *Diabetes* 2005; **54**: 2328–2335.
8. Thomas ME, Schreiner GF. Contribution of proteinuria to progressive renal injury: consequences of tubular uptake of fatty acid bearing albumin. *Am J Nephrol* 1993; **13**: 385–398.
9. Kamijo A, Kimura K, Sugaya T *et al.* Urinary free fatty acids bound to albumin aggravate tubulointerstitial damage. *Kidney Int* 2002; **62**: 1628–1637.
10. Thomas ME, Harris KP, Walls J *et al.* Fatty acids exacerbate tubulointerstitial injury in protein-overload proteinuria. *Am J Physiol Renal Physiol* 2002; **283**: F640–F647.
11. Risdon RA, Sloper JC, De Wardener HE. Relationship between renal function and histological changes found in renal-biopsy specimens from patients with persistent glomerular nephritis. *Lancet* 1968; **2**: 363–366.
12. Dreyer C, Krey G, Keller H *et al.* Control of the peroxisomal beta-oxidation pathway by a novel family of nuclear hormone receptors. *Cell* 1992; **68**: 879–887.
13. Schoonjans K, Staels B, Auwerx J. Role of the peroxisome proliferator-activated receptor (PPAR) in mediating the effects of fibrates and fatty acids on gene expression. *J Lipid Res* 1996; **37**: 907–925.
14. Aoyama T, Peters JM, Iritani N *et al.* Altered constitutive expression of fatty acid-metabolizing enzymes in mice lacking the peroxisome proliferator-activated receptor alpha (PPARalpha). *J Biol Chem* 1998; **273**: 5678–5684.
15. Braissant O, Foufelle F, Scotto C *et al.* Differential expression of peroxisome proliferator-activated receptors (PPARs): tissue distribution of PPAR-alpha, -beta, and -gamma in the adult rat. *Endocrinology* 1996; **137**: 354–366.
16. Deji N, Kume S, Araki S *et al.* Structural and functional changes in the kidneys of high-fat diet-induced obese mice. *Am J Physiol Renal Physiol* 2009; **296**: F118–F126.

17. Nagai Y, Nishio Y, Nakamura T *et al.* Amelioration of high fructose-induced metabolic derangements by activation of PPARalpha. *Am J Physiol Endocrinol Metab* 2002; **282**: E1180–E1190.
18. Koh E, Kim M, Park J *et al.* Peroxisome proliferator-activated receptor (PPAR)-alpha activation prevents diabetes in OLETF rats: comparison with PPAR-gamma activation. *Diabetes* 2003; **52**: 2331–2337.
19. Shin S, Lim J, Chung S *et al.* Peroxisome proliferator-activated receptor-alpha activator fenofibrate prevents high-fat diet-induced renal lipotoxicity in spontaneously hypertensive rats. *Hypertens Res* 2009; **32**: 835–845.
20. Park C, Zhang Y, Zhang X *et al.* PPARalpha agonist fenofibrate improves diabetic nephropathy in db/db mice. *Kidney Int* 2006; **69**: 1511–1517.
21. Perico N, Codreanu I, Schieppati A *et al.* Pathophysiology of disease progression in proteinuric nephropathies. *Kidney Int Suppl* 2005; **67**: S79–S82.
22. Kamijo Y, Hora K, Kono K *et al.* PPARalpha protects proximal tubular cells from acute fatty acid toxicity. *J Am Soc Nephrol* 2007; **18**: 3089–3100.
23. Sugiyama M, Kinoshita K, Kishimoto K *et al.* Deletion of IL-18 receptor ameliorates renal injury in bovine serum albumin-induced glomerulonephritis. *Clin Immunol* 2008; **128**: 103–108.
24. Ishigaki N, Yamamoto T, Shimizu Y *et al.* Involvement of glomerular SREBP-1c in diabetic nephropathy. *Biochem Biophys Res Commun* 2007; **364**: 502–508.
25. Fan C, Pan J, Usuda N *et al.* Steatohepatitis, spontaneous peroxisome proliferation and liver tumors in mice lacking peroxisomal fatty acyl-CoA oxidase. Implications for peroxisome proliferator-activated receptor alpha natural ligand metabolism. *J Biol Chem* 1998; **273**: 15639–15645.
26. Zhao Z, Lee YJ, Kim SK *et al.* Rosiglitazone and fenofibrate improve insulin sensitivity of pre-diabetic OLETF rats by reducing malonyl-CoA levels in the liver and skeletal muscle. *Life Sci* 2009; **84**: 688–695.
27. Toyama T, Nakamura H, Harano Y *et al.* PPARalpha ligands activate antioxidant enzymes and suppress hepatic fibrosis in rats. *Biochem Biophys Res Commun* 2004; **324**: 697–704.
28. Guerre-Millo M, Rouault C, Poulain P *et al.* PPAR-alpha-null mice are protected from high-fat diet-induced insulin resistance. *Diabetes* 2001; **50**: 2809–2814.
29. Keech A, Simes R, Barter P *et al.* Effects of long-term fenofibrate therapy on cardiovascular events in 9795 people with type 2 diabetes mellitus (the FIELD study): randomised controlled trial. *Lancet* 2005; **366**: 1849–1861.
30. Guerre-Millo M, Gervois P, Raspé E *et al.* Peroxisome proliferator-activated receptor alpha activators improve insulin sensitivity and reduce adiposity. *J Biol Chem* 2000; **275**: 16638–16642.
31. Jeong S, Han M, Lee H *et al.* Effects of fenofibrate on high-fat diet-induced body weight gain and adiposity in female C57BL/6J mice. *Metabolism* 2004; **53**: 1284–1289.
32. Bahlmann FH, Song R, Boehm SM *et al.* Low-dose therapy with the long-acting erythropoietin analogue darbepoetin alpha persistently activates endothelial Akt and attenuates progressive organ failure. *Circulation* 2004; **110**: 1006–1012.
33. Bligh E, Dyer W. A rapid method of total lipid extraction and purification. *Can J Biochem Physiol* 1959; **37**: 911–917.
34. Kume S, Haneda M, Kanasaki K *et al.* SIRT1 inhibits transforming growth factor beta-induced apoptosis in glomerular mesangial cells via Smad7 deacetylation. *J Biol Chem* 2007; **282**: 151–158.
35. Takaya K, Koya D, Isono M *et al.* Involvement of ERK pathway in albumin-induced MCP-1 expression in mouse proximal tubular cells. *Am J Physiol Renal Physiol* 2003; **284**: F1037–F1045.